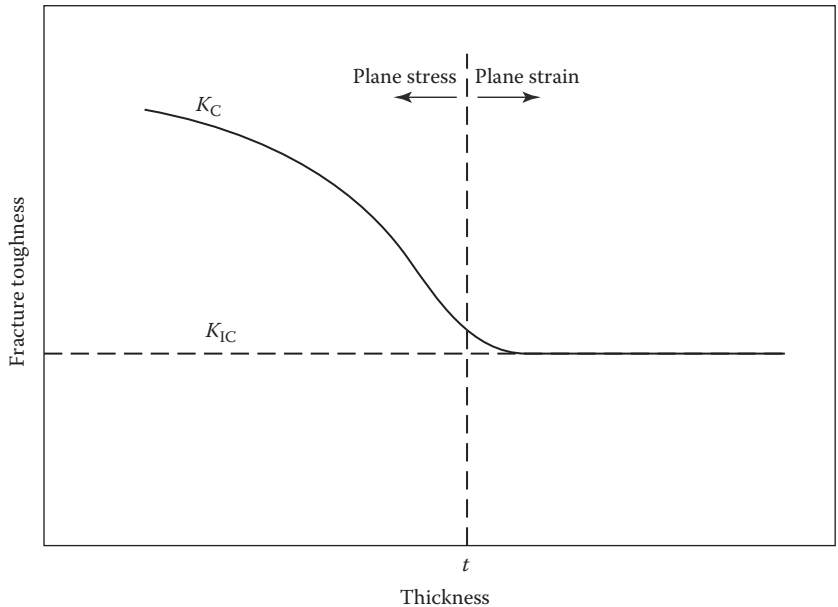

Figure 2.1 Effect of thickness on fracture toughness behavior.

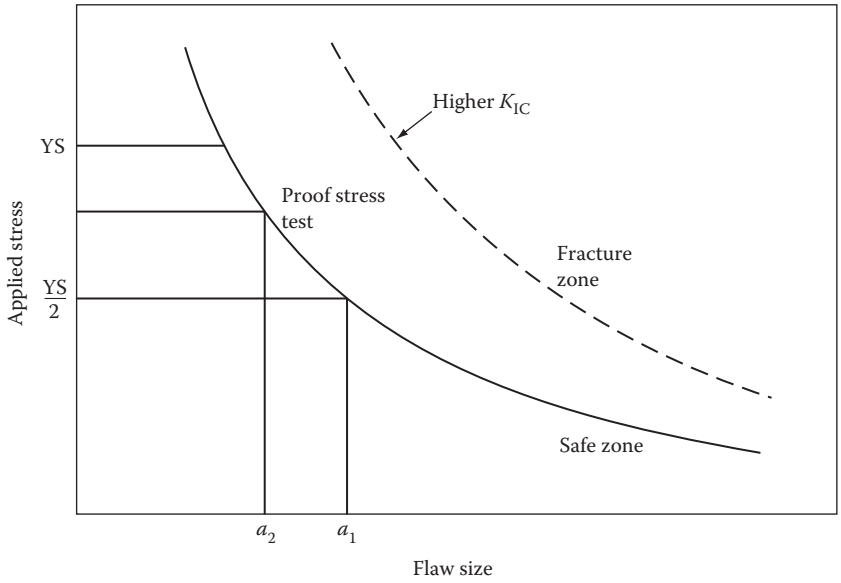

Figure 2.2 Schematic relationship between stress, flaw size, and fracture toughness.

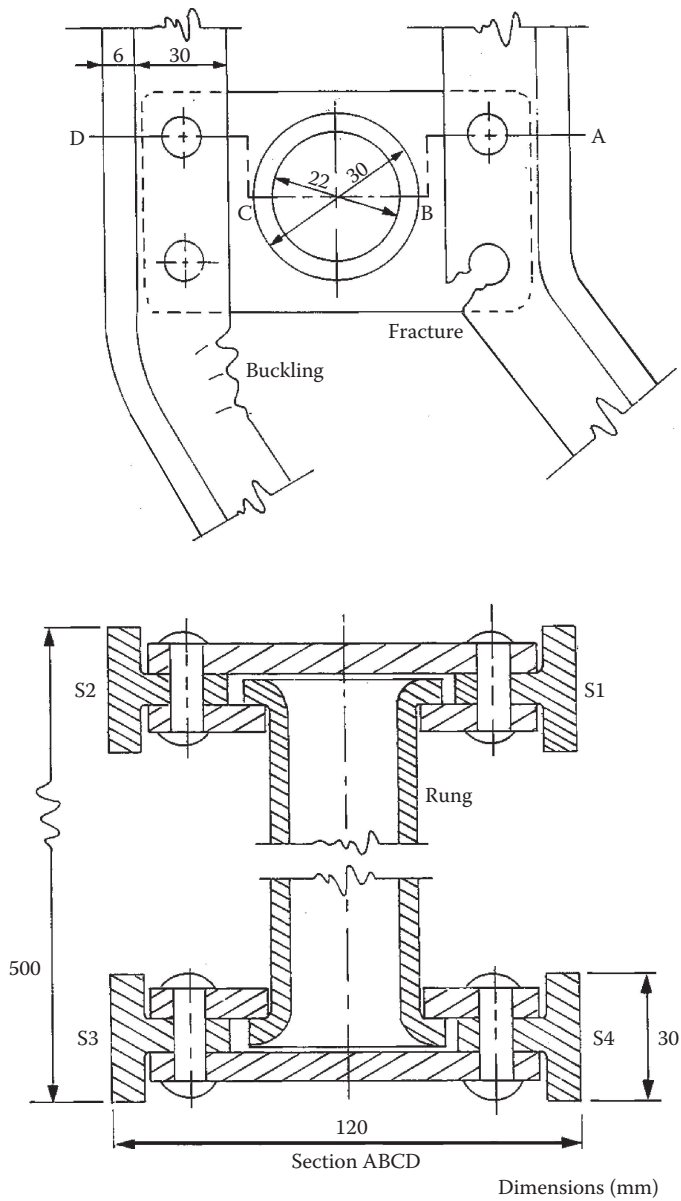

Figure 2.3 Failure of an aluminum ladder.

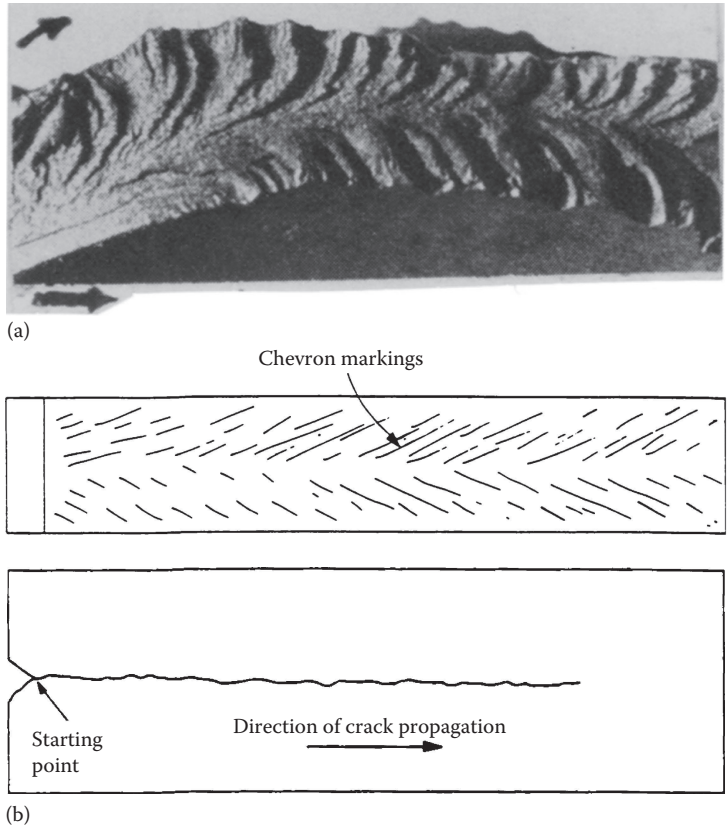

Figure 2.4 Chevron patterns in brittle fracture. (a) Chevron markings in steel. (From Rollason, E.C., *Metallurgy for Engineers*, 4th edn., Edward Arnold, London, U.K., 1977.) (b) Schematic representation.

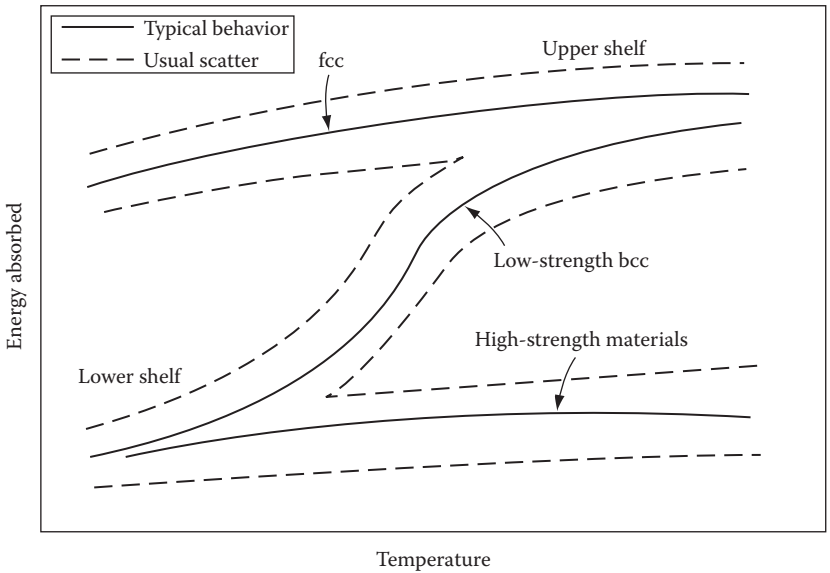

Figure 2.5 Schematic representation of the effect of temperature on the energy absorbed in fracture.

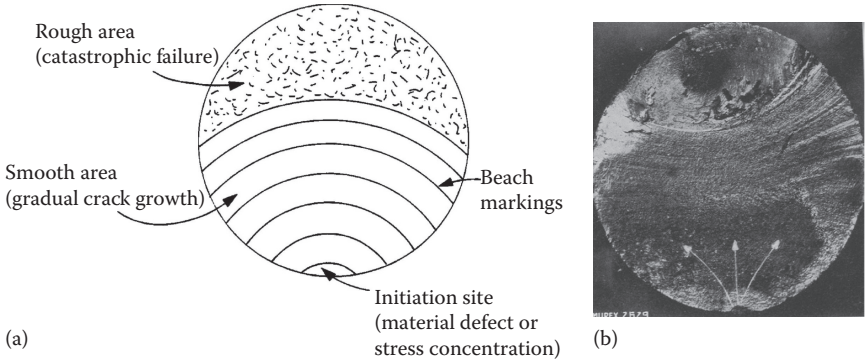

Figure 2.6 General appearance of a fatigue fracture surface. (a) Schematic representation; (b) fatigue fracture of automobile axle shaft. (From Rollason, E.C., *Metallurgy for Engineers*, 4th edn., Edward Arnold, London, U.K., 1977.)

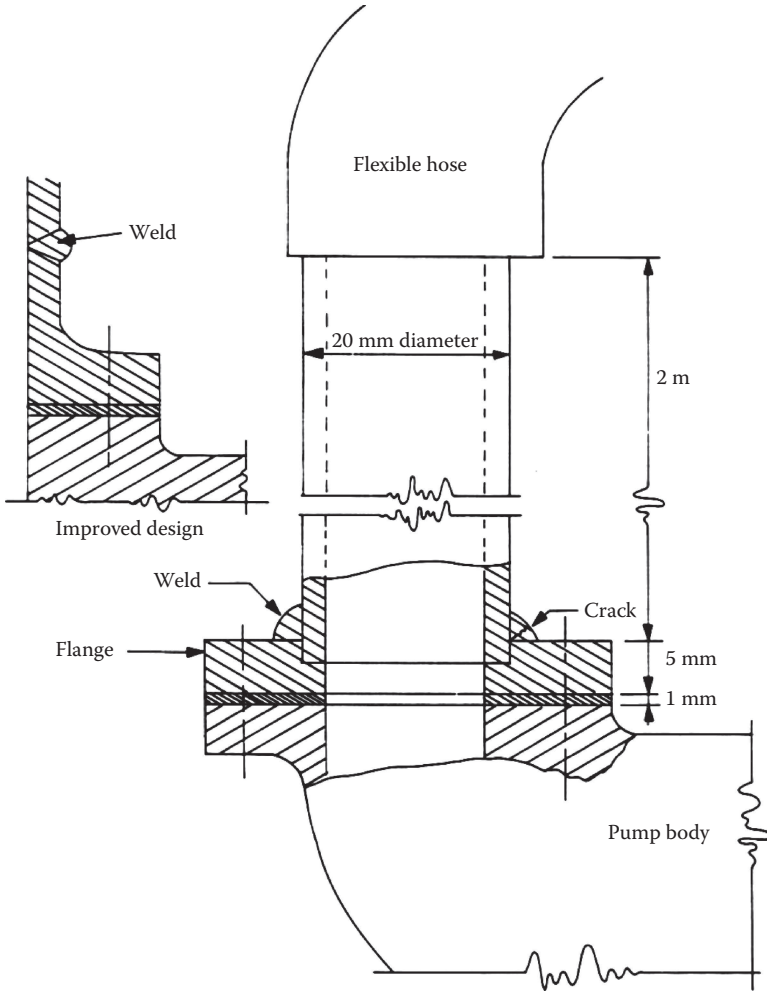

Figure 2.7 Failure of pressure line of a hydraulic pump.

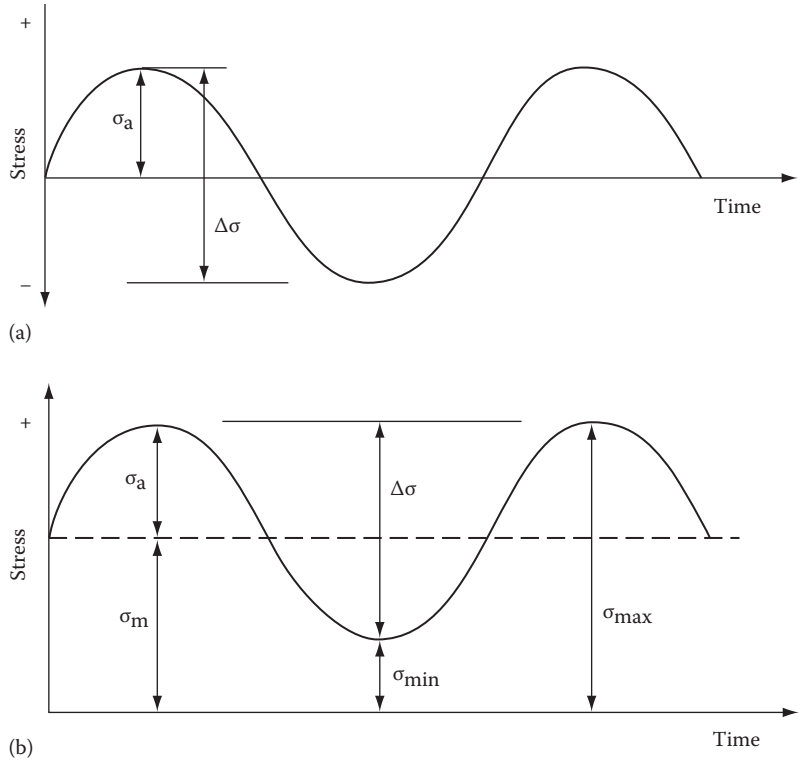

Figure 2.8 Types of fatigue loading. (a) Alternating stress, $R = -1$; (b) fluctuating stress.

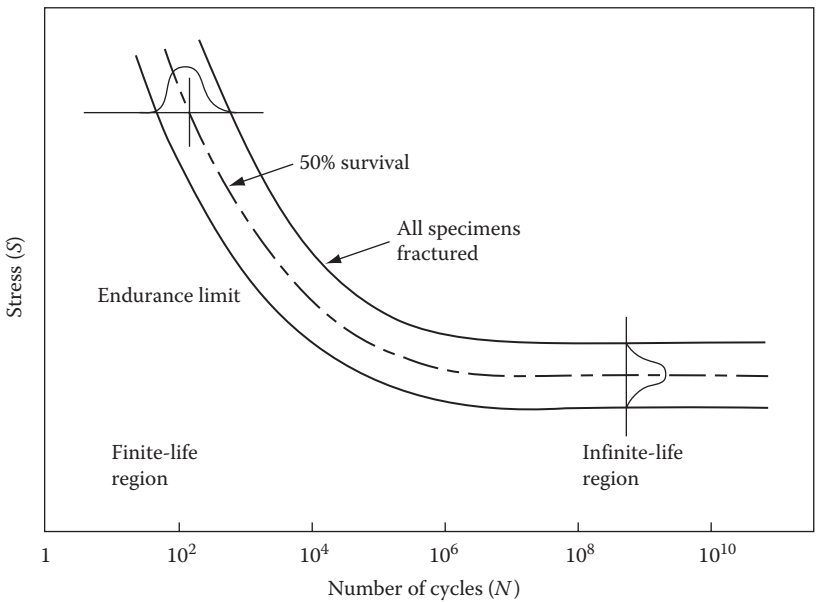

Figure 2.9 Representation of fatigue test results on the *S*–*N* curve.

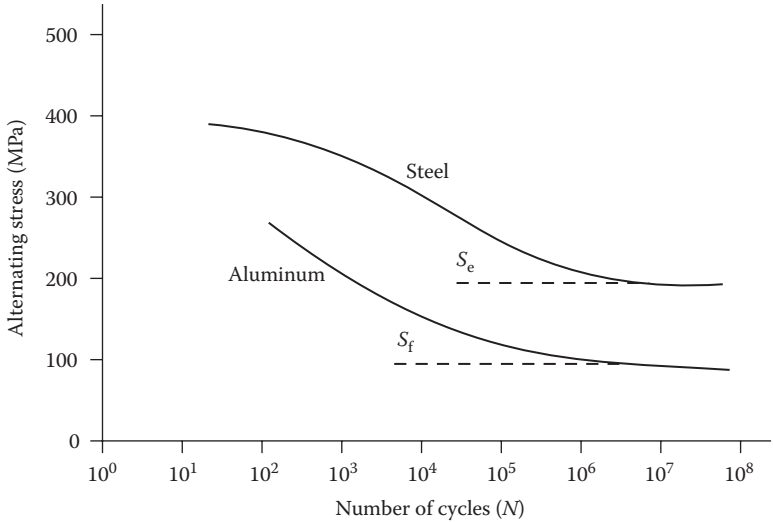

Figure 2.10 Fatigue results as represented by the *S*–*N* curves. Steel exhibits an endurance limit and its curve levels off at S_e. Aluminum does not exhibit an endurance limit, and its curve continues to decline for all values of *N*.

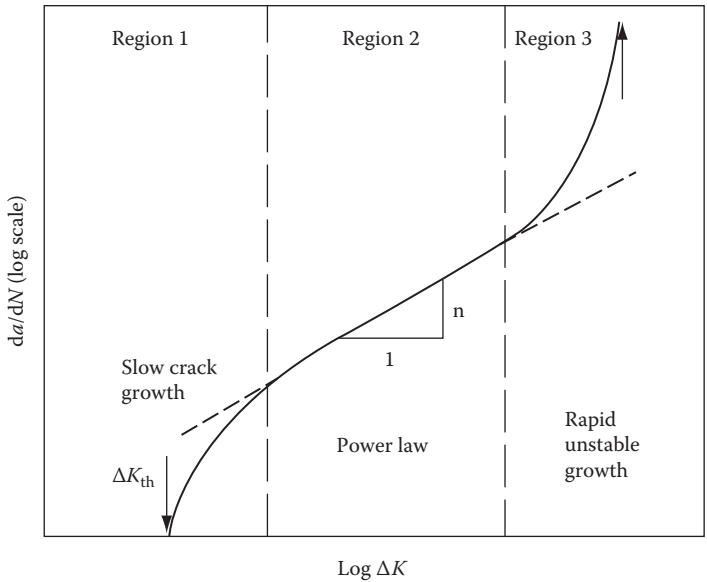

Figure 2.11 Schematic illustration of the effect of the range of the stress intensity factor (ΔK_I) on fatigue-crack growth rate (da/dN).

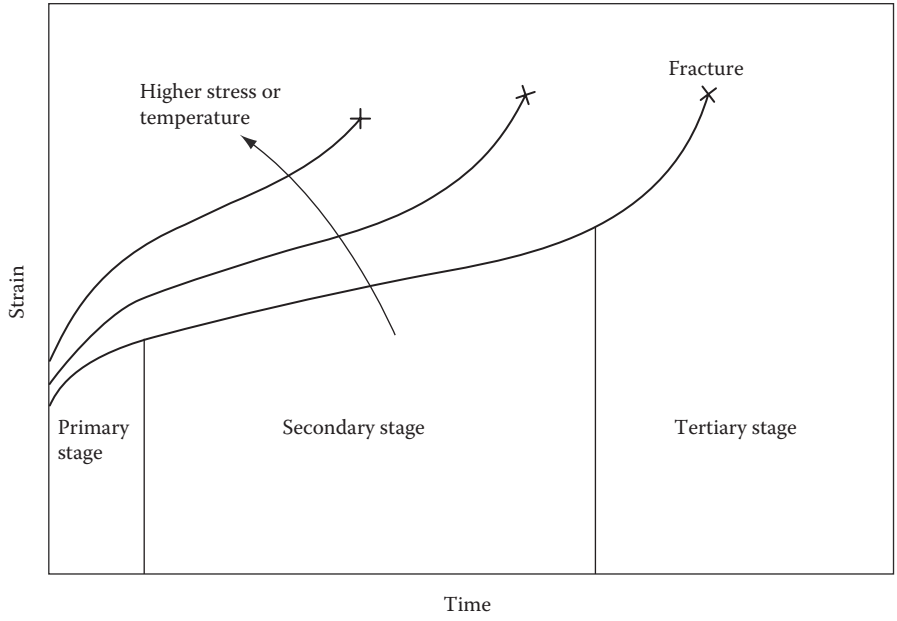

Figure 2.12 Schematic creep curve under tensile loading.

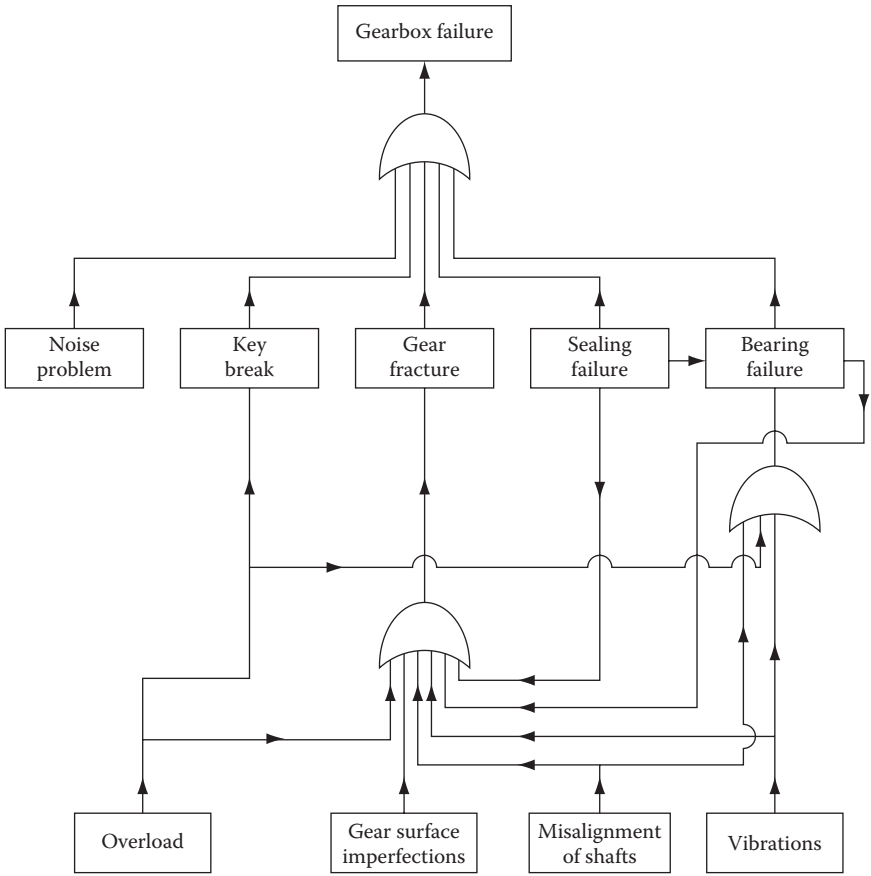

Figure 2.13 Simple analysis of a gearbox failure.

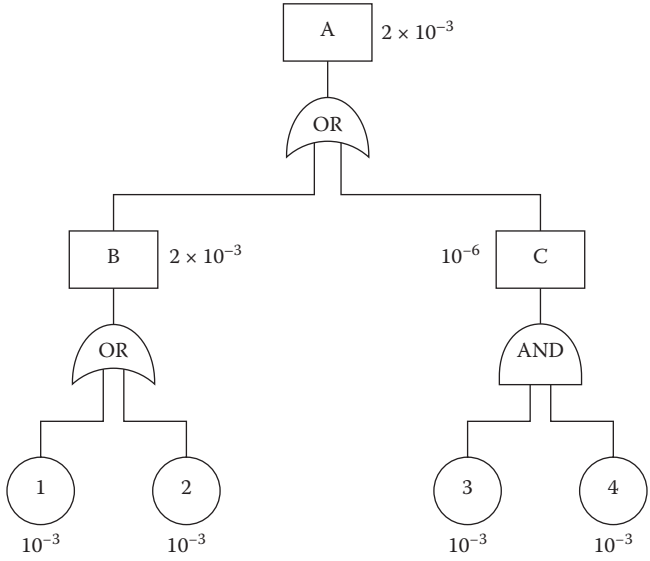

Figure 2.14 Sensitivity of system reliability to probabilities of failure of various components. Numbers beside each event represent probabilities.

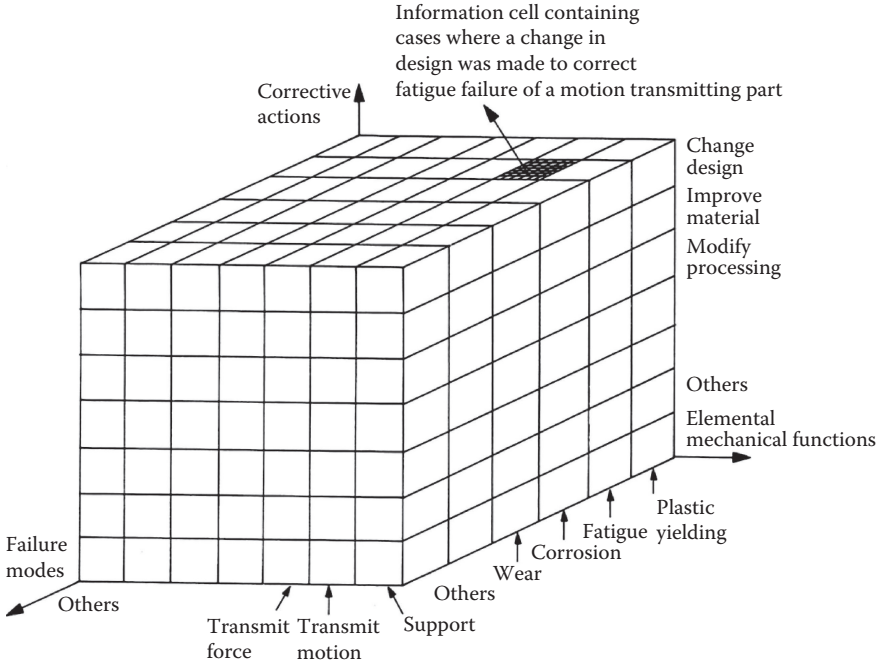

Figure 2.15 Part of failure experience matrix, which can be used to store failure information.